

High sensitivity detection of NO₂ and NH₃ in air using chemical vapor deposition grown graphene

Cite as: Appl. Phys. Lett. **100**, 203120 (2012); <https://doi.org/10.1063/1.4720074>

Submitted: 05 January 2012 . Accepted: 04 May 2012 . Published Online: 18 May 2012

Fazel Yavari, Eduardo Castillo, Hemtej Gullapalli, Pulickel M. Ajayan, and Nikhil Koratkar



View Online



Export Citation

ARTICLES YOU MAY BE INTERESTED IN

Sub-ppt gas detection with pristine graphene

Applied Physics Letters **101**, 053119 (2012); <https://doi.org/10.1063/1.4742327>

Enhanced sensitivity of graphene ammonia gas sensors using molecular doping

Applied Physics Letters **108**, 033106 (2016); <https://doi.org/10.1063/1.4940128>

Gas sensing in 2D materials

Applied Physics Reviews **4**, 021304 (2017); <https://doi.org/10.1063/1.4983310>

Meet the Next Generation
of Quantum Analyzers

And Join the Launch
Event on November 17th



Register now



Zurich
Instruments



High sensitivity detection of NO₂ and NH₃ in air using chemical vapor deposition grown graphene

Fazel Yavari,¹ Eduardo Castillo,¹ Hemtej Gullapalli,² Pulickel M. Ajayan,² and Nikhil Koratkar^{1,3,a)}

¹*Department of Mechanical, Aerospace and Nuclear Engineering, Rensselaer Polytechnic Institute, Troy, New York 12180, USA*

²*Department of Mechanical and Materials Engineering, Rice University, Houston, Tennessee 77105, USA*

³*Department of Materials Science and Engineering, Rensselaer Polytechnic Institute, Troy, New York 12180, USA*

(Received 5 January 2012; accepted 4 May 2012; published online 18 May 2012)

We show that graphene films synthesized by chemical-vapor-deposition enables detection of trace amounts of nitrogen dioxide (NO₂) and ammonia (NH₃) in air at room temperature and atmospheric pressure. The gas species are detected by monitoring changes in electrical resistance of the graphene film due to gas adsorption. The sensor response time was inversely proportional to the gas concentration. Heating the film expelled chemisorbed molecules from the graphene surface enabling reversible operation. The detection limits of ~ 100 parts-per-billion (ppb) for NO₂ and ~ 500 ppb for NH₃ obtained using our device are markedly superior to commercially available NO₂ and NH₃ detectors. © 2012 American Institute of Physics. [<http://dx.doi.org/10.1063/1.4720074>]

Detection of hazardous gases such as NH₃ and NO₂ is a crucial task in many situations such as chemical processing, environmental and emissions monitoring, as well as detection of explosives.^{1–3} At levels higher than 1 parts-per-million (ppm) in air, NO₂ and NH₃ can cause severe damage to human respiration systems and lung tissues.² Therefore the development of on-site chemical sensors that can detect these gases at the sub-ppm level is an essential step towards controlling the level of these gases in the environment as well as in chemical processes.

Graphene, an atomic layer of carbon atoms arranged in a honeycomb hexagonal lattice, has a very high specific surface area, and its electrical properties are extremely sensitive^{1–3} to low traces of NH₃ and NO₂. The sensitivity, response time, and reversibility of graphene sensors depend mainly on the graphene synthesis method, the detection mode, and the gas species being sensed. Different types of graphene sheets such as hydrazine-reduced graphene oxide,^{4,5} mechanically exfoliated graphene,⁶ thermally reduced graphene oxide,⁷ epitaxially grown graphene,⁸ and macro-scale three-dimensional (3D) graphene foams³ have been previously used as chemical sensors. Although detection of individual molecules of NH₃ and NO₂ using mechanically exfoliated graphene has been achieved,⁶ the fabrication process for these sensors involves tedious efforts for mechanical cleavage of graphite and the results can be very different from sample to sample. Other techniques usually lead to ppm level detection of NH₃ and NO₂ gases. For example, using hydrazine-reduced graphene oxide with different levels of reduction, NH₃ and NO₂ gases were detected down to about 5 ppm in air.¹ Thermally reduced graphene oxide⁷ is capable of detecting NO₂ down to 2 ppm. A 3D network of graphene sheets (graphene foam³) was also used to detect 20 ppm of NH₃ and NO₂ in air. Finally, epitaxially grown

graphene can lead to detection of 2.5 ppm of NO₂ in air.⁸ Therefore sub-ppm level detection of NH₃ and NO₂ using graphene has proved to be challenging.

Among different fabrication methods of graphene, chemical-vapor-deposition (CVD) is a very promising technique towards mass production of high quality graphene with uniform thickness. However, there are few studies on the response of CVD-grown graphene to adsorption of gases.⁹ In this work, high-quality CVD-grown graphene has been used to detect NH₃ and NO₂ at the sub-ppm level in air at room temperature and atmospheric pressure. The response time is comparable to other graphene based sensors; however, heating the graphene film to $\sim 200^\circ\text{C}$ was necessary to expel the chemisorbed NO₂ and NH₃ species and achieve reversible operation. Due to the small size of these sensors, they can be mass-produced from a large wafer containing a single sheet of CVD-grown graphene that is patterned into smaller pieces and electrically addressed using lithography. This can potentially lead to practical sensor devices that are suitable for sub-ppm level detection of NH₃ and NO₂ in mixtures with air at room temperature and atmospheric pressure.

Graphene samples were synthesized by CVD on copper (Cu) foils using hexane as a liquid precursor as demonstrated in our previous work.^{10,11} Cu foils are selected here since precipitation of carbon on Cu is a self-limiting process which allows for deposition of very thin films. To transfer the graphene film from Cu on to an insulating silicon (Si)/silicon-dioxide (SiO₂) substrate, a thin poly(methyl methacrylate) (PMMA) film was coated on the graphene/Cu system. Next, the underlying Cu substrate was dissolved in dilute nitric acid, and the graphene/PMMA film was transferred onto a Si substrate with a ~ 300 -nm-thick insulating SiO₂ layer. After the transfer was complete, the PMMA layer was dissolved away using acetone to leave only the graphene film on the Si/SiO₂ substrate. Any trace PMMA remaining on the graphene film was evaporated by heating the samples to $\sim 375^\circ\text{C}$ in a furnace with constant argon-hydrogen flow and holding the

^{a)} Author to whom correspondence should be addressed. Electronic mail: koratn@rpi.edu.

temperature for ~ 1 h. Next, photolithography followed by e-beam evaporator deposition was used to pattern four electrodes (titanium (Ti)/gold (Au), 3/30 nm) on the top surface of the transferred graphene film. Note that the very thin ~ 3 nm Ti layer was used to promote adhesion between the Au contacts and the graphene surface. As indicated in the optical micrograph of Fig. 1(a), the electrodes were deposited at four points to form a Van Der Pauw configuration.¹⁰ The size of the graphene film that is enclosed within the electrode pattern is $\sim 30 \mu\text{m} \times 16 \mu\text{m}$. Raman spectroscopy (using 514 nm wavelength excitation) was used to examine the number of graphene layers within the film. Typical results are shown in Fig. 1(b) and indicate the Raman D, G, and 2D peaks at ~ 1350 , 1584 , and $\sim 2675 \text{ cm}^{-1}$, respectively. Based on the ratio of the integrated intensity of the 2D and G peaks,¹² it is clear that in some places the film is monolayer graphene while in some locations bi-layer graphene is also present.

Silver epoxy (EJ-2189 two part kit from EPOXY Technology) was used to bond four Au wires to the contact pads on the graphene film. These wires were in turn connected to four leads of a chip carrier, making it possible to electrically address the sample. The graphene device was placed in an environmental chamber with electrical feed-through, and air was pumped out of the chamber to establish a high vacuum ($\sim 10^{-6}$ Torr). The horizontal and vertical resistances¹⁰ associated with the Van Der Pauw configuration were measured in real-time using a Labview data acquisition system and used to compute the graphene sheet resistance. Once the baseline graphene sheet resistance was determined, NO_2 gas

pre-mixed with air at the appropriate concentration was released into the chamber. All tests were performed at room temperature and atmospheric pressure. Figure 2(a) shows that the graphene sheet resistance decreases markedly as NO_2 molecules adsorb onto the graphene film surface. The magnitude of the resistance change decreases as the NO_2 concentration is reduced from 200 to 0.1 ppm (i.e., 100 ppb). We expect that since NO_2 is a strong oxidizing agent, it will attract electrons from the graphene, thereby increasing the number of conducting holes. This hole (or p-type doping) shifts the Fermi level closer to the valence band causing increase in the graphene sheet conductance. After the resistance change had stabilized in about 50 min, we established vacuum desorption conditions and heated the samples using a hot plate to $\sim 200^\circ\text{C}$ in order to desorb the NO_2 molecules from the graphene film surface. As can be seen in Fig. 2(a), the graphene sheet resistance recovers close to its original value as a result of the heating which indicates that the device can be operated in a reversible manner. Figure 2(b) shows the sensor response time which is the time taken for the graphene resistance change to reach $\sim 90\%$ of the steady state value. The sensor response time is shown at each value of the NO_2 concentration; the results indicate that the response time of the device is inversely dependent on the NO_2 concentration. This is to be expected since at lower concentrations it will take longer for the NO_2 molecules to equilibrate on the graphene film surface. We also show in Fig. 2(b) the percentage decrease in the graphene sheet resistance

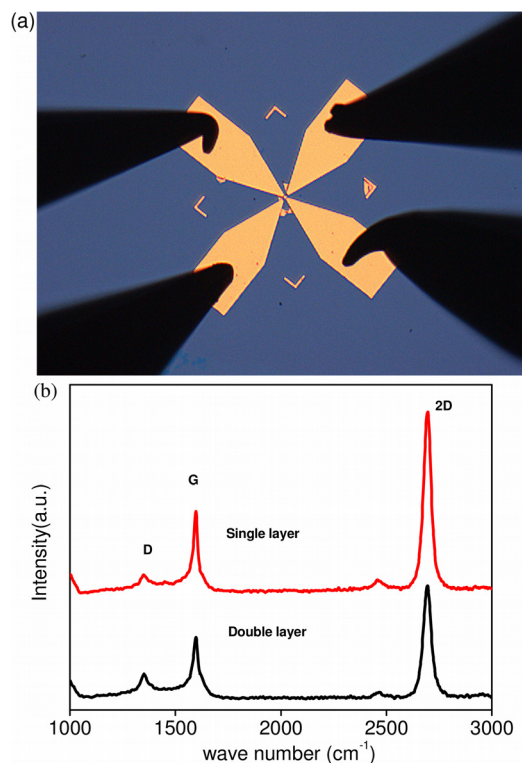


FIG. 1. Synthesis of the graphene device. (a) Optical micrograph of graphene film grown by CVD on Cu and then transferred onto a Si/SiO₂ substrate. Gold contact pads in the Van Der Pauw configuration were deposited on the film. (b) Typical Raman spectra obtained from different locations on the graphene film indicating that the film is comprised of single and bi-layer graphene.

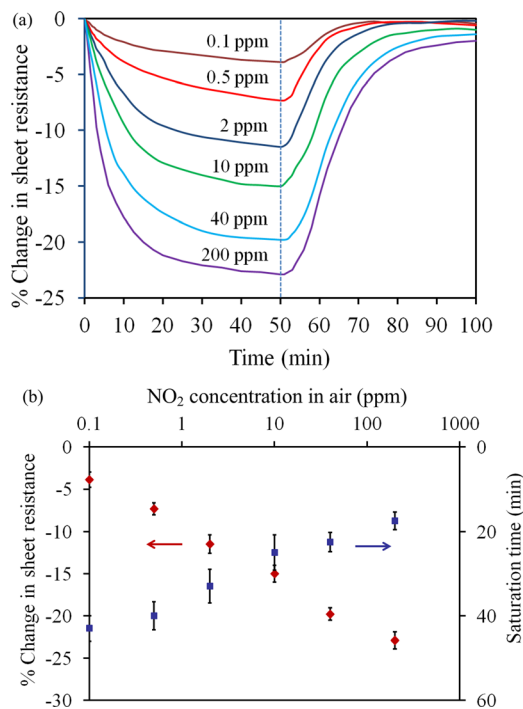


FIG. 2. NO_2 detection at room temperature and atmospheric pressure. (a) Percentage reduction in the graphene sheet resistance as a function of time for various NO_2 concentrations. After ~ 50 min the samples were exposed to vacuum desorption conditions and heated to $\sim 200^\circ\text{C}$ using a hot plate resulting in recovery of the graphene sheet resistance close to its baseline level. (b) The device sensitivity (i.e., the steady state percentage change in the graphene sheet resistance) and the sensor response or saturation time (i.e., time taken for the graphene sheet resistance change to reach $\sim 90\%$ of steady state) are plotted as a function of the NO_2 concentration.

as a function of the NO_2 concentration. The sheet resistance change drops from $\sim 23\%$ to $\sim 4\%$ as the NO_2 concentration is brought down from 200 to 0.1 ppm. The sensitivity of our graphene device is impressive in comparison to commercially available NO_2 detectors. For instance commercial polypyrrole conducting polymer sensors can detect ~ 1000 ppm of NO_2 by a $\sim 10\%$ resistance change at room temperature.^{13,14} The CVD-grown graphene device developed in this work shows comparable resistance change at room temperature at four orders of magnitude lower NO_2 concentration.

Next we investigated the sensor's response for NH_3 detection at room temperature and atmospheric pressure. Figure 3(a) shows time traces for resistance change of the graphene device on exposure to various concentrations of NH_3 ranging from ~ 1000 to ~ 0.5 ppm. For this case, the graphene sheet resistance increases sensitively due to the adsorption of NH_3 molecules to the film surface. Note that graphene under ambient conditions is observed to display p-type behavior¹⁵ due to the electron withdrawing nature of adsorbed water or oxygen moieties. Setting up gold contacts on graphene has also been shown to p-dope the graphene.¹⁶ NH_3 being a reducing agent will donate electrons to the p-type graphene, thereby reducing the conductance. As before vacuum desorption conditions in conjunction with substrate heating to $\sim 200^\circ\text{C}$ was used to expel chemisorbed NH_3 molecules from the graphene surface causing the graphene sheet resistance to recover close to its original value (Fig. 3(a)). Interestingly for the case of NH_3 we find that the time taken for the resistance change to stabilize is much

larger compared to NO_2 detection (Fig. 3(b)) and ranges from 120 to 300 min depending on the gas concentration. Figure 3(b) also depicts the percentage rise in the graphene sheet resistance as a function of the NH_3 concentration. The sheet resistance change varies from $\sim 90\%$ to $\sim 3\%$ as the NH_3 concentration is brought down from ~ 1000 to ~ 0.5 ppm. This represents a dramatic increase in the device sensitivity as compared to commercially available electrical resistivity based NH_3 detectors. For instance conducting polymer sensors¹⁷ undergo $\sim 30\%$ resistance change when exposed to 10 000 ppm of NH_3 at room temperature. The CVD-grown graphene detector developed here exhibits comparable changes in resistivity at 3–4 orders of magnitude lower NH_3 concentrations.

We checked the stability of our sensor device by repeated testing over several months. The sensor was kept exposed to the ambient environment during this period. Typical results for 1000 ppm detection of NH_3 are shown in Fig. S1 of the supplemental material.¹⁸ Over four months of testing, the graphene device showed consistent results. We also investigated the response of our graphene device to gas species that are commonly found in air such as carbon dioxide (CO_2) and humidity. Typically the concentration of CO_2 in air is 0.03%–0.04%. Figure S2 in the supplemental material¹⁸ shows the change in electrical resistance of the sheet when exposed to 0.04% of CO_2 . As can be seen in the plot the change in electrical resistance induced by CO_2 adsorption to the surface is minimal ($<0.01\%$). Humidity however did have a stronger effect on the sensor response. The humidity testing was performed in an environmental chamber with precise control of the humidity level. At room temperature and 50% relative humidity, the graphene sheet shows $\sim 5\%$ increase in resistivity (Fig. S3 in the supplemental material¹⁸). This increase in sheet resistivity is caused by the breaking of the sublattice and molecular symmetries of graphene by the adsorbed water molecules, which opens up a band gap in graphene.¹⁰ However the graphene's sensitivity to humidity should not affect its ability to detect NO_2 and NH_3 as adsorption of these gases will cause a further change in its resistivity with respect to the new baseline value (in the presence of humidity).

To summarize, we have shown the effectiveness of CVD grown graphene as a sensor device for ultra-sensitive (sub-ppm level) detection of important analytes such as NO_2 and NH_3 in mixtures with air at room temperature and atmospheric pressure. The devices could be reversibly used by desorbing the adsorbed gas species by heating to $\sim 200^\circ\text{C}$ using a hot plate under vacuum. The device is also able to distinguish between NO_2 and NH_3 since in the former case the conductance is increased due to gas adsorption while for the latter the conductance decreases. In addition to providing high sensitivity of gas detection, the advantage of CVD grown graphene is that it is amenable to deposition on large area substrates and can be lithographically patterned to create a dense array of sensor elements which can find use in Lab-on-Chip and other miniaturized sensor applications.

N.K. acknowledges funding support from the US Office of Naval Research (Award No. N000140910928) and the US National Science Foundation (Award No. 0900188).

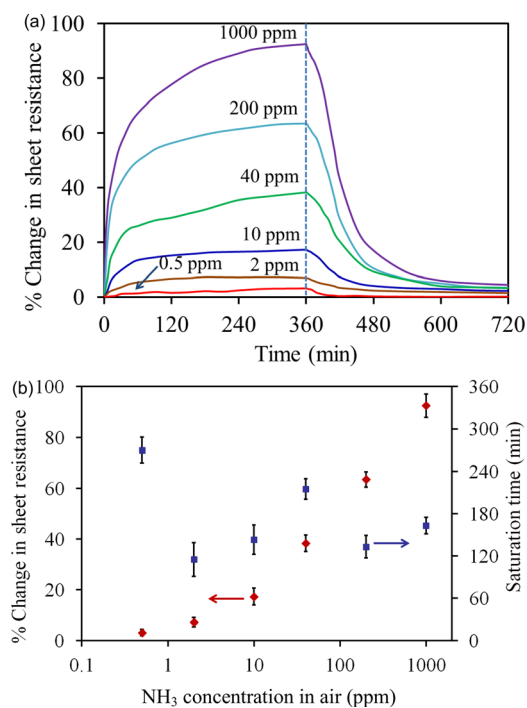


FIG. 3. NH_3 detection at room temperature and atmospheric pressure. (a) Percentage increase in graphene sheet resistance as a function of time for various NH_3 concentrations. After ~ 360 min the samples were exposed to vacuum desorption conditions and heated to $\sim 200^\circ\text{C}$ using a hot plate resulting in recovery of the graphene sheet resistance. (b) The device sensitivity and the sensor response or saturation time are plotted as a function of the NH_3 concentration.

- ¹J. D. Fowler, M. J. Allen, V. C. Tung, Y. Yang, R. B. Kaner, and B. H. Weiller, *ACS Nano* **3**, 301 (2009).
- ²L. Hsu, T. Ativanichayaphong, H. Cao, J. Sin, M. Graff, H. E. Stephanou, and J. Chiao, *Sens. Rev.* **27**, 121 (2007).
- ³F. Yavari, Z. Chen, Z. A. V. Thomas, W. Ren, H.-M. Cheng, and N. Koratkar, *Sci. Rep.* **1**, 166 (2011).
- ⁴J. T. Robinson, F. K. Perkins, E. S. Snow, Z. Q. Wei, and P. E. Sheehan, *Nano Lett.* **8**, 3137 (2008).
- ⁵G. H. Lu, S. Park, K. H. Yu, R. S. Ruoff, L. E. Ocola, D. Rosenmann, and J. H. Chen, *ACS Nano* **5**, 1154 (2011).
- ⁶F. Schedin, A. K. Geim, S. V. Morozov, E. W. Hill, P. Blake, M. I. Katsnelson, and K. S. Novoselov, *Nat. Mater.* **6**, 652 (2007).
- ⁷G. Lu, L. E. Ocola, and J. Chen, *Appl. Phys. Lett.* **94**, 083111 (2009).
- ⁸R. Pearce, T. Iakimov, M. Andersson, L. Hultman, A. L. Spetz, and R. Yakimova, *Sens. Actuators B* **155**, 451 (2011).
- ⁹W. Wu, Z. Liu, L. A. Jauregui, Q. Yu, R. Pillai, H. Cao, J. Bao, Y. P. Chen, and S.-S. Pei, *Sens. Actuators B* **150**, 296 (2010).
- ¹⁰F. Yavari, C. Kritzing, C. Gaire, L. Song, H. Gulapalli, T. Borca-Tasciuc, P. M. Ajayan, and N. Koratkar, *Small* **6**, 2535 (2010).
- ¹¹P. Dhiman, F. Yavari, X. Mi, H. Gullapalli, Y. Shi, P. M. Ajayan, and N. Koratkar, *Nano Lett.* **11**, 3123 (2011).
- ¹²A. Gupta, G. Chen, P. Joshi, S. Tadigadapa, and P. C. Eklund, *Nano Lett.* **6**, 2667 (2006).
- ¹³J. Miasik, A. Hooper, and B. Tofield, *J. Chem. Soc. Faraday Trans. 1* **82**, 1117 (1986).
- ¹⁴Y. Shimizu and M. Egashira, *MRS Bull.* **24**, 18 (1999).
- ¹⁵J. Moser, A. Verdaguer, D. Jimenez, A. Barreiro, and A. Bachtold, *Appl. Phys. Lett.* **92**, 123507 (2008).
- ¹⁶Y. Ren, S. Chen, W. Cai, Y. Zhu, C. Zhu, and R. S. Ruoff, *Appl. Phys. Lett.* **97**, 053107 (2010).
- ¹⁷G. Sberveglieri, S. Groppelli, and P. Nelli, *Sens. Actuators B* **4**, 457 (1991).
- ¹⁸See supplementary material at <http://dx.doi.org/10.1063/1.4720074> for long term stability of the sensor device, for sensitivity of the sensor to carbon dioxide, and for sensitivity of the sensor to humidity.